

INFLUENCE OF THE SOIL PROPERTIES ON CRATERS PRODUCED BY EXPLOSIONS ON THE SOIL SURFACE

Daniel Ambrosini^{*}, Bibiana Luccioni[†], and Rodolfo Danesi[†]

^{*} Facultad de Ingeniería, Universidad Nacional de Cuyo
Centro Universitario - Parque Gral. San Martín - (5500) Mendoza. Fax 54 0261 4380120
e-mail: dambrosini@uncu.edu.ar, web page: <http://fing.uncu.edu.ar/>

[†] Instituto de Estructuras
Facultad de Ciencias Exactas y Tecnología, Universidad Nacional de Tucumán
Av. Roca 1800, 4000 Tucumán, Argentina. Tel.: 54-0381-4364087 Fax: 0381 4364087
e-mail: bluccioni@herrera.unt.edu.ar, web page: <http://herrera.unt.edu.ar/iest>

Key words: Craters, explosion, blast waves, soils, hydrocode.

Abstract. *In case of terrorist attacks or other intentional actions using explosives, it is extremely important the information that can be obtained from the crater generated by the blast waves. For example, the focus of the explosion and the mass of the explosive used in the attack can be deduced examining the location and dimensions of the crater. However, studies about craters produced by explosions on or above ground level, which would be the case when the explosive charge is situated in a vehicle, are rarely found in the open technical literature. In a previous paper, a numerical study related to crater produced by explosive loads located on the soil surface was presented. In this paper, a study about the influence of the variability of the soil properties on the crater dimensions is presented.*

The numerical model as well as the analysis procedure were validated against experimental observations of the crater diameters. Results of numerical tests performed with different amounts of explosive on the soil surface are presented. Moreover, the effect of elevation of the center of energy release of explosive loads located on the soil surface is analyzed and discussed. Simple prediction equations for the crater diameter are presented.

1 INTRODUCTION

Blasting loads have come to be forefront of attention in recent years due to a number of accidental and intentional events that affected important structures all over the world, clearly indicating that this issue is important for purposes of structural design and reliability analysis. In consequence, extensive research activities in the field of blast loads have taken place in the last few decades.

Dynamic loads due to explosions result in strain rates of the order of 10^{-1} to 10^3 s^{-1} which imply short time dynamic behaviour of the materials involved, characterised mainly by a great overstrength and increased stiffness, in comparison with normal, static properties. In the case of soils, the response and the mechanism of crater formation are particularly complex due to the usual anisotropy and non linear nature of the material, and to the variability of mechanical properties and coexistence of the three phases: solid, liquid and gaseous. Generally, simplifying assumptions must be made in order to solve specific problems. Until now, most practical problems have been solved through empirical approaches. Years of industrial and military experience have been condensed in charts or equations (Baker et al.¹, Smith and Hetherington²). These are useful tools, for example, to establish the explosive weight to yield a perforation of certain dimensions or to estimate the type and amount of explosive used in a terrorist attack, from the damage registered. Most research is related to underground explosions and only a few papers are concerned with explosions at ground level. Studies about craters produced by explosions above ground level, which would be the case when the explosive charge is situated in a vehicle, are rarely found in the open technical literature. Some reports are classified and access is limited to government agencies.

Most of the information about explosively formed craters found in the literature is based on experimental data. Numerical studies were scarce until recently.

However, with the rapid development of computer hardware over the last years, it has become possible to make detailed numerical simulations of explosive events in personal computers, significantly increasing the availability of these methods. New developments in integrated computer hydrocodes complete the tools necessary to carry out the numerical analysis successfully. Nevertheless, it is important to be aware that both these models and analysis procedures still need experimental validation.

In a previous paper³, a numerical study related to crater produced by explosive loads located on the soil surface was presented. In this paper, a study about the influence of the variability of the soil properties on the crater dimensions is presented. The analysis is performed with a hydrocode and material models and analysis procedures are validated with experimental results. The effect of elevation of the center of energy release of explosive loads located on the soil surface is analyzed and discussed. All the results are compared with empirical equations used nowadays for the prediction of crater dimensions and new simple equations are proposed.

2 THEORY AND PREVIOUS RESULTS

2.1 Crater formation

A crater produced by an explosive charge situated on or above the ground level is schematized in Figure 1. The crater dimensions defined by Kinney and Graham⁴ are used in this paper (Figure 1): D is the apparent crater diameter, D_r is the actual crater diameter and H_2 is the apparent depth of the crater. The depth of the crater created by an explosion ordinarily is about one quarter of the diameter of the crater, but this ratio depends on the type of soil involved. The diameter of the crater produced by an explosion also depends on the relative location of the explosive charge to the ground level. Thus, explosions above surface level may not create any crater at all (Kinney and Graham⁴).

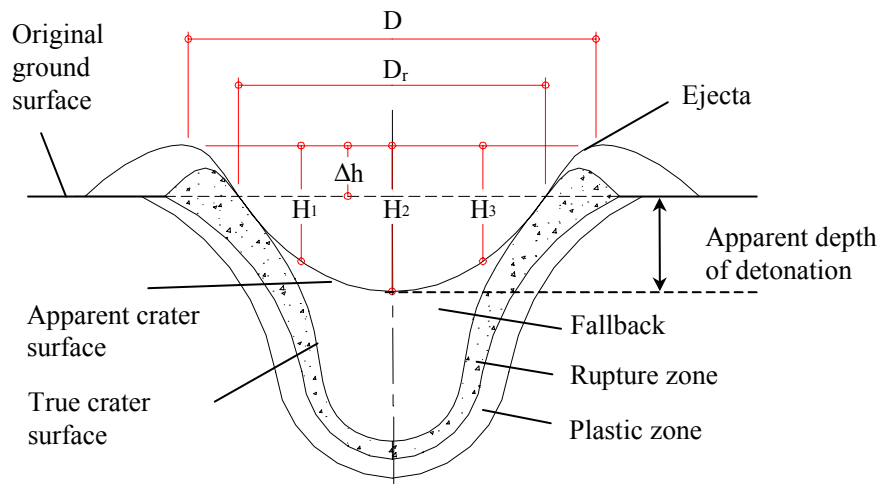


Figure 1: Definitions of the crater dimensions

Tests of crater formation are appropriate tools to study the blast phenomena, the behaviour and destructive power of different explosives and the response of soils and rocks under this type of load (Persson et al.⁵). The mechanism of crater formation is complex and it is related to the dynamic physical properties of air, soil and soil-air interface. Even very carefully performed cratering tests give deviations in the dimensions measured of the order of 10% , while differences of as much as 30% to 40% are common (Bull et al.⁶)

A cavity is always formed when a confined explosion is produced in a mass of soil. If the explosion is close to the surface, a crater is formed and a complex interaction between gravity effects, soil strength and transient load conditions takes place. The most important variables in defining the crater shape and size are the mass W of the explosive and the depth of the detonation beneath the air/soil interface d . When $d < 0$, the explosive is detonated over the air/soil interface, $d = 0$ when the detonation occurs in the air/soil interface and $d > 0$ when the explosive is detonated beneath the soil surface. For $d > 0$, the crater mechanism is altered by gravitational effects. When the depth of the detonation increases, larger amounts of subsoil

must be expelled by the explosion. Thus, the crater radius and the depth of the crater increase when d increases, until a certain limit value, from which they rapidly decrease (Bull et al.⁶).

Studies concerned with the characteristics of craters caused by explosions usually resort to dimensional analysis and statistics. The scaling law establishes that any linear dimension “L” of the crater can be expressed as a constant multiplied by W^α divided by the distance of the charge from the ground, where W represents the equivalent TNT mass of explosive and α is a coefficient that is dependent on whether the gravitational effects can be neglected or not. When the gravitational effects can be neglected the cubic root law is applicable ($\alpha = 0.33$) and in the other cases the functional dependence can be quite complex.

Baker et al.⁷ present a dimensional study to model the crater formation phenomenon in the case of underground explosions. Six parameters are chosen to define the problem: the explosive mass W , the depth of the explosive charge d , the apparent crater radius R , the soil density ρ , and two strength parameters to define the soil properties: one with the dimensions of stress σ , related to soil strength, and the other with the dimensions of a force divided by a cubic length (Nm^{-3}) K , that takes into account gravitational effects.

After a dimensional analysis and many empirical observations, the following functional relation may be obtained (Baker et al.⁷).

$$\frac{R}{d} = f \left(\frac{W^{7/24}}{\sigma^{1/6} K^{1/8} d} \right) \quad (1)$$

If $\frac{R}{d}$ (scaled radius of the crater) is plotted as a function of $W^{7/24}/d$ (Baker et al.⁷), it can be seen that this relation is close to experimental results and can be approximately simplified by two straight lines, one with a moderate slope for $W^{7/24}/d > 0.3$ and one steeper for $W^{7/24}/d < 0.3$. For $W^{7/24}/d < 0.3$, the scaled radius of the crater is sensitive to small changes in the independent parameter and, due to this fact, the independent parameter or the scaled radius may exhibit great variability. Experimental conditions are better controlled for $W^{7/24}/d > 0.3$.

The preceding paragraphs refer to underground explosions. There is less information about explosions at ground level. Statistical studies of about 200 accidental above-ground explosions of relative large magnitude are presented by Kinney and Graham⁴. The results exhibit a variation coefficient in the crater diameter of about 30%. From these results, the following empirical equation for the crater diameter was proposed.

$$D [m] = 0.8W[Kg]^{1/3} \quad (2)$$

Additional experimental evidence was obtained during the surface explosions performed by EMRTC (Energetic Materials Research Center of the Mineralogical and Technologic Institute of New Mexico). EMRTC conducted experimental determinations to explore

alternative ways of controlling the blasting power. In this program, the explosion of 250kg of TNT situated at ground level formed a 3.8m diameter crater.

In connection with the morphological and structural types of the craters, Melosh⁸ determine four different basic types: (a) bowl-shaped, (b) flat-floored with central uplift, (c) flat floored with a peak ring and (d) flat floored with >2 asymmetric rings (multiring basins). One of the factors that determine the shape is the height of burst. On the other hand, numerical and independent research results presented by Iturrioz et al.⁹ preliminary confirm the formation of the same shapes of craters. Additionally, there are important contributions in the literature related to cratering studies, but many of them are about predicting *rock* damage, ex. Yang et al.¹⁰, Liu and Katsabanis¹¹ and Wu et al.¹² and others are related with *buried* explosions, ex. Wang and Lu¹³ and Zhou et al.¹⁴.

2.2 Experimental tests

In a previous paper, Ambrosini et al.¹⁵ presented the results of a series of tests performed with different amounts of explosive at short distances above and below ground level, as well as on the soil surface. These results were used in this paper to calibrate the soil parameters of the numerical model as well as to validate the analysis procedure. The description of the test will be summarised in this point.

The tests were performed in a large flat region, without rock formations, normally used for agriculture. Two exploratory drillings and two test pits were used to determine the mechanical properties of the soil. The exploratory holes were drilled to depths of 2m and 5m, respectively, with standard penetration tests (SPT) performed at 1m intervals. The test pits were dug to a depth of 2m in order to collect undisturbed soil samples for triaxial testing and for a more precise determination of the in situ density. Partial results of the soil tests are presented in Table 1. The soil profile was quite uniform in the entire 40x50m testing area, being characterized by:

- 1) 0 to 0.70m Brown clayey silt with organic matter.
- 2) 0.70 to 5.0 m Reddish brown clayey silt of low plasticity, classification CL, very dry.

The crater tests were performed in a selected 40m x 50m area. A grid with 10m spacing was used to locate the explosive charges at its nodes. Each row of the grid corresponded to loads of the same magnitude. Charges equivalent to 1, 2, 4, 7 and 10 kg of TNT were located on the five rows. All the charges were spherical. In the first two columns, the explosives were situated tangential to the surface. In the following columns, the explosives were located 0.5m above ground level. Finally, in the last two columns, the loads were situated 1m above ground level and 1m underground respectively. The charges above ground level were located hanging on wood tripods. The explosive used in the tests was Gelamón 80, a NG based gelatinous explosive theoretically equivalent in mass to 80% TNT.

Table 1: Soil properties of experimental tests – Drilling S-1

Depth [m]	Free water level	Type of soil	SPT tests		WD t/m ³	DD t/m ³	w	T200	LL %	PI %	Clas. /UCS
			Depth [m]	N							
0.7	without free water surface	(1)	0.5-1.0	6	1.25	1.14	9.6	87	28.1	12.3	CL
1.0			1.5-2.0	12	1.43	1.27	12.7	91	27.9	8.6	CL
2.0		(2)					19.3	95	31.0	10.4	CL
3.0											
5.0								End of the drilling			

WD: Wet density, DD: Dry density, w: Moisture content, T200: Percentage that passes through sieve N°200, LL: Liquid limit, PI: Plastic index, Clas. /UCS: Classification according UCS

The following comments apply to the crater size measurement procedure:

- a) The apparent crater diameter D (Figure 1) was measured in all cases according to the definition given by Kinney and Graham³
 - b) 3 measurements of the crater diameter and 3 of the crater depth were performed.
 - c) In general, the craters produced by explosives situated at ground level presented a small mound in the center formed by the loose soil that fell down on the site after the explosion.
 - d) The shape of most of the craters was flat-floored with central uplift.
- As illustration, the crater due to a surface explosion is shown in Figure 2. The results about the dimensions of the craters are presented in Ambrosini et al.¹⁵.



Figure 2: Superficial explosion crater obtained in a test

3 NUMERICAL MODEL

3.1 Introduction and numerical tool

Computer codes normally referred as “hydrocodes” encompass several different numerical techniques in order to solve a wide variety of non-linear problems in solid, fluid and gas dynamics. The phenomena to be studied with such a program can be characterized as highly time dependent with both geometric non-linearities (e.g. large strains and deformations) and material non-linearities (e.g. plasticity, failure, strain-hardening and softening, multiphase equations of state). Different numerical tools are used in some papers in order to solve similar problems of crater determination. For example ABAQUS (Yang et al.¹⁰), AUTODYN (Wu et al.¹², Wang and Lu¹³), SALE2D (Baratoux and Melosh¹⁶, Nolan et al.¹⁷) and CTH (Pierazzo and Melosh¹⁸).

In this paper, the program AUTODYN-2D¹⁹, which is a “hydrocode” that uses finite difference, finite volume, and finite element techniques to solve a wide variety of non-linear problems in solid, fluid and gas dynamics, is used. The phenomena to be studied with such a program can be characterized as highly time dependent with both geometric non-linearities (e.g. large strains and deformations) and material non-linearities (e.g. plasticity, failure, strain-hardening and softening, multiphase equations of state).

The various numerical processors available in AUTODYN generally use a coupled finite difference/finite volume approach similar to that described by Cowler and Hancock²⁰. This scheme allows alternative numerical processors to be selectively used to model different components/regimes of a problem. Individual structured meshes operated on by these different numerical processors can be coupled together in space and time to efficiently compute structural, fluid, or gas dynamics problems including coupled problems (e.g. fluid-structure, gas-structure, structure-structure, etc.).

AUTODYN includes the following numerical processors: Lagrange, Euler, ALE, Shell, Euler-Godunov, Euler-FCT and SPH. All the above processors use explicit time integration. The first-order Euler approach scheme is based upon the method developed by Hancock²¹.

While finite element codes are usually based on the equilibrium condition, the hydrocode utilizes the differential equations governing unsteady material dynamic motion: the local conservation of mass, momentum and energy. In order to obtain a complete solution, in addition to appropriate initial and boundary conditions, it is necessary to define a further relation between the flow variables. This can be found from a material model, which relates stress to deformation and internal energy (or temperature). In most cases, the stress tensor may be separated into a uniform hydrostatic pressure (all three normal stresses equal) and a stress deviatoric tensor associated with the resistance of the material to shear distortion.

The relation between the hydrostatic pressure, the local density (or specific volume) and local specific energy (or temperature) is known as an equation of state. Since solids are able to withstand a certain amount of tensile stress, it is necessary to consider extending the equations of state into limited regions of negative values of the pressure (tension). However, since the analytic forms derived for ranges of positive pressure it may not be valid for extrapolation into

the negative regions special attention should be paid in using some forms of equation of state. The *hydrodynamic tensile limit*, sometimes referred to as p_{min} , is the minimum pressure to which the material can sustain continuous expansion. If the material pressure drops below this limit in a cell it is assumed that the material will fracture, or in some way lose its uniform and continuous ability to sustain a tensile pressure. This would then form the lower limit of the analytic equation of state. Regardless the definition of a value of p_{min} it may be necessary to provide a different analytic form for negative pressure values from that used for positive values (but taking care to ensure continuity of function and derivatives at $p = 0$).

While there are many problems that can be calculated using a hydrodynamic equation of state, there are many applications where material strength effects (i.e. its resistance to shearing forces) cannot be ignored and indeed may even dominate. If the material is solid and has finite shear strength then, in addition to the calculation of the hydrostatic pressure, it is necessary to define relations between shear stress and strain. The methodology followed in this paper is that first one formulated by Wilkins²² to extend conventional numerical hydrodynamic codes to include the effects of material strength and resistance to shear distortion.

A relation to define the transition between elastic and plastic strain, both in compression and release, and a relation to define the onset of fracture, are also required. The yield criterion governing the transition from elastic to plastic behaviour may involve only constant yield strength, or this strength may itself be a function of the degree of strain (work hardening), the rate of strain and/or the temperature of the material (energy dependency).

Real materials are not able to withstand tensile stresses that exceed the material local tensile strength. The computation of the dynamic motion of materials assuming that they always remain continuous, even if the predicted local stresses reach very large negative values, will lead to unphysical solutions. For this reason the model has to be constructed to recognize when tensile limits are reached, to modify the computation to deal with this and to describe the properties of the material after this formulation has been applied.

3.2 Numerical mesh

In this paper, an Euler formulation is used to model both air and soil. In the Euler processors, a control volume method is used to solve the equations that govern conservation of mass, momentum, and energy. The integral and discrete forms of these equations are expressed in conservation form to obtain accurate, stable solutions. Terms producing changes in conserved variables are divided into two groups: Lagrangian or transport (convective). A two-step numerical procedure is used to solve the finite-difference equations. In the first step, the Lagrange step, the Lagrangian form of the equations are updated or advanced one time interval (time step). In the second step, the Euler step, the updated variables are mapped onto the Euler mesh. Multiple materials are handled through either a volume fraction technique or an interface technique originally developed by Youngs²³. All variables are cell centered. This allows arbitrary shaped control volumes to be formed more readily at the interface between Euler and Lagrange grids, facilitating the computation of fluid-structure or gas-structure interaction problems.

The use of symmetry conditions allows using a two-dimensional (2D) mesh considering axial symmetry. The number of cells required to produce accurate solutions is greatly reduced when compared with a full 3D model. The mesh used for explosive charges situated on the ground level is shown in Figure 3a. The mesh was filled with different materials: air, TNT and soil as indicated in Figure 3b.

In case of charges of 1 to 10 kg of TNT a mesh of 6m x 12.5m was used. However, in case of charges of 50 kg of TNT or greater, a mesh of 10m x 12.5m was used.

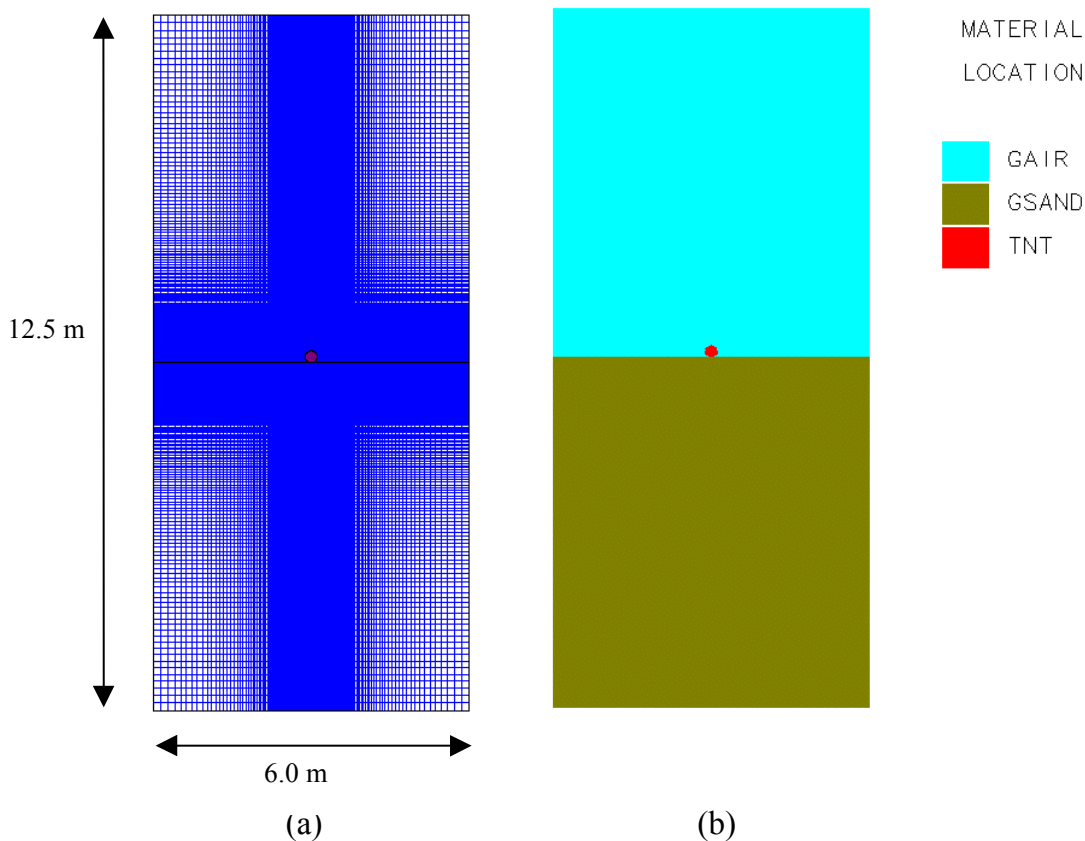


Figure 3: Numerical model for explosives charges situated on the ground level. a) Mesh b) Material location

3.3 Materials models

All the terms in the equations presented in this section could be in any congruent system units, but the SI units is recommended.

a) *Air*: The ideal gas equation of state was used for the air. This is one of the simplest forms of equation of state for gases. In an ideal gas, the internal energy is a function of the temperature alone and if the gas is polytropic the internal energy is simply proportional to temperature. It follows that the equation of state for a gas, which has uniform initial conditions, may be written as,

$$p = (\gamma - 1)\rho e \quad (3)$$

in which p is the hydrostatic pressure, ρ is the density and e is the specific internal energy. γ is the adiabatic exponent, it is a constant (equal to $1 + R/c_v$) where constant R may be taken to be the universal gas constant R_0 divided by the effective molecular weight of the particular gas and c_v is the specific heat at constant volume. The values of the constants used for air are presented in Ambrosini et al.³

b) *TNT*: High explosives are chemical substances which, when subject to suitable stimuli, react chemically very rapidly (in order of microseconds) releasing energy. In the hydrodynamic theory of detonation, this very rapid time interval is shrunk to zero and a detonation wave is assumed to be a discontinuity which propagates through the unreacted material instantaneously liberating energy and transforming the explosive into detonating products. The normal Rankine-Hugoniot relations, expressing the conservation of mass, momentum and energy across the discontinuity may be used to relate the hydrodynamic variables across the reaction zone. The only difference between the Rankine-Hugoniot equations for a shock wave in a chemically inert material and those for a detonation wave is the inclusion of a chemical energy term in the energy conservation equation.

Since the 1939-45 war, when there was naturally extensive study of the behaviour of high explosives, there has been a continuous attempt to understand the detonation process and the performance of the detonation products, leading to considerable improvements in the equation of state of the products. The most comprehensive form of equation of state developed over this period, the "Jones - Wilkins - Lee" (JWL) equation of state, is used in this paper.

$$p = C_1 \left(1 - \frac{\omega}{r_1 v} \right) e^{-r_1 v} + C_2 \left(1 - \frac{\omega}{r_2 v} \right) e^{-r_2 v} + \frac{\omega e}{v} \quad (4)$$

Where $v = 1/\rho$ is the specific volume, C_1 , r_1 , C_2 , r_2 and ω (adiabatic constant) are constants and their values have been determined from dynamic experiments and are available in the literature for many common explosives. The values used for TNT are presented in Ambrosini et al.³

It can be shown that at large expansion ratios the first and second terms on the right hand side of Equation (4) become negligible and hence the behaviour of the explosive tends towards that of an ideal gas. Therefore, at large expansion ratios, where the explosive has expanded by a factor of approximately 10 from its original volume, it is valid to switch the equation of state for a high explosive from JWL to ideal gas. In such a case the adiabatic exponent for the ideal gas, γ , is related to the adiabatic constant of the explosive, ω , by the relation $\gamma = \omega + 1$. The reference density for the explosive can then be modified and the material compression will be reset. Potential numerical difficulties are therefore avoided.

An explosion may be initiated by various methods. However, whether an explosive is dropped, thermally irradiated or shocked, either mechanically or from a shock from an initiator (of more sensitive explosive), initiation of an explosive always goes through a stage in which a shock wave is an important feature. Lee-Tarver equation of state (Lee and Tarver²⁴) was used to model both the detonation and expansion of TNT in conjunction with JWL EOS

to model the unreacted explosive.

c) Soil: A shock equation of state combined with an elastoplastic strength model based on Mohr Coulomb criterion and an hydro tensile limit were used for the soil.

A Mie-Gruneisen form of equation of state based on the shock Hugoniot was used. The Rankine-Hugoniot equations for the shock jump conditions can be regarded as defining a relation between any pair of the variables ρ , p , e , u_p (material velocity behind the shock) and U (shock velocity). In many dynamic experiments it has been found that for most solids and many liquids over a wide range of pressure there is an empirical linear relationship between u_p and U .

$$U = c_0 + s u_p \quad (5)$$

in which c_0 is the initial sound speed and s a dimensionless parameter.

This is the case even up to shock velocities around twice the initial sound speed c_0 and shock pressures of order 100 GPa. In this case the equation of state is:

$$p = p_H + \Gamma \rho (e - e_H) \text{ with } p_H = \frac{\rho_0 c_0^2 \mu (1 + \mu)}{[1 - (s - 1)\mu]^2}; \quad e_H = \frac{1}{2} \frac{p_H}{\rho_0} \frac{\mu}{1 + \mu}; \quad \mu = \frac{\rho}{\rho_0} - 1 \quad (6)$$

where p is the hydrostatic pressure, ρ_0 is the initial density, e is the specific internal energy and Γ is the Gruneisen Gamma parameter and it is assumed that $\Gamma \rho = \Gamma_0 \rho_0 = \text{const}$

An elastoplastic model with Mohr Coulomb yield criterion was used for the strength effects. This model is an attempt to reproduce the behaviour of dry soil where the cohesion and compaction result in an increasing resistance to shear up to a limiting value of yield strength as the loading increases. This is modelled by a piecewise linear variation of yield stress with pressure. In tension (negative values of p) soils have little tensile strength and this is modelled by dropping the curve for $Y(p)$ rapidly to zero as p goes negative to give a realistic value for the limiting tensile strength.

A non associated flow rule (Prandtl-Reuss type) that avoids the problem of shear induced dilatancy in soils was used. A constant hydrodynamic tensile limit was specified as failure criterion. All the material properties used initially for the soil model are presented in Ambrosini et al.³.

4 INFLUENCE OF THE SOIL PROPERTIES

4.1 Crater formation and wave propagation

The process of crater formation for a spherical explosive load of 10 kg of TNT lying on the ground is illustrated in Figure 4. It may be observed that it takes about 10 ms for the hole crater to be formed. Moreover, the wave propagation in the air and the soil is illustrated in Figure 5a and 5b. Finally, in Figure 5c, the Von Mises stresses developed in the soil are shown at 1.17 ms for the case of 50 kg of TNT with the energy release center at the ground level.

4.2 Comparison with experimental results

In order to validate not only the material models and material properties but also the analysis procedures, a comparison with experimental results was first performed. The results of a series of tests performed with different amounts of explosive from 1kg to 10kg of TNT on the soil surface (Ambrosini et al.¹⁵) were used to calibrate the materials parameters.

In this section, the properties of the soil incorporated in the numerical model are obtained from real properties of the soil at the test site (see Ambrosini et al.¹⁵ and Table 1). Then, the initial density is adopted 1250 kg/m³. The value of the Shear Modulus G can be obtained from the SPT test by using the empirical relationship (7a) given by Ohsaki and Iwasaki²⁵ for sands or, alternatively, the expression (7b) given by Hara et al.²⁶ for cohesive soils.

$$G_o = 12N^{0.8} MPa \quad (7a)$$

$$G_o = 15.8N^{0.67} MPa \quad (7b)$$

For the soils founded at the test site, the bounds are given by the expression (7a): $G = 50$ to 88 MPa. A value of 70 Mpa was adopted. Some authors disagree with to use SPT results in order to obtain elastic properties of the soil. However, below it will be shown that the variation of the Shear Modulus does not affect the dimensions of the crater significantly.

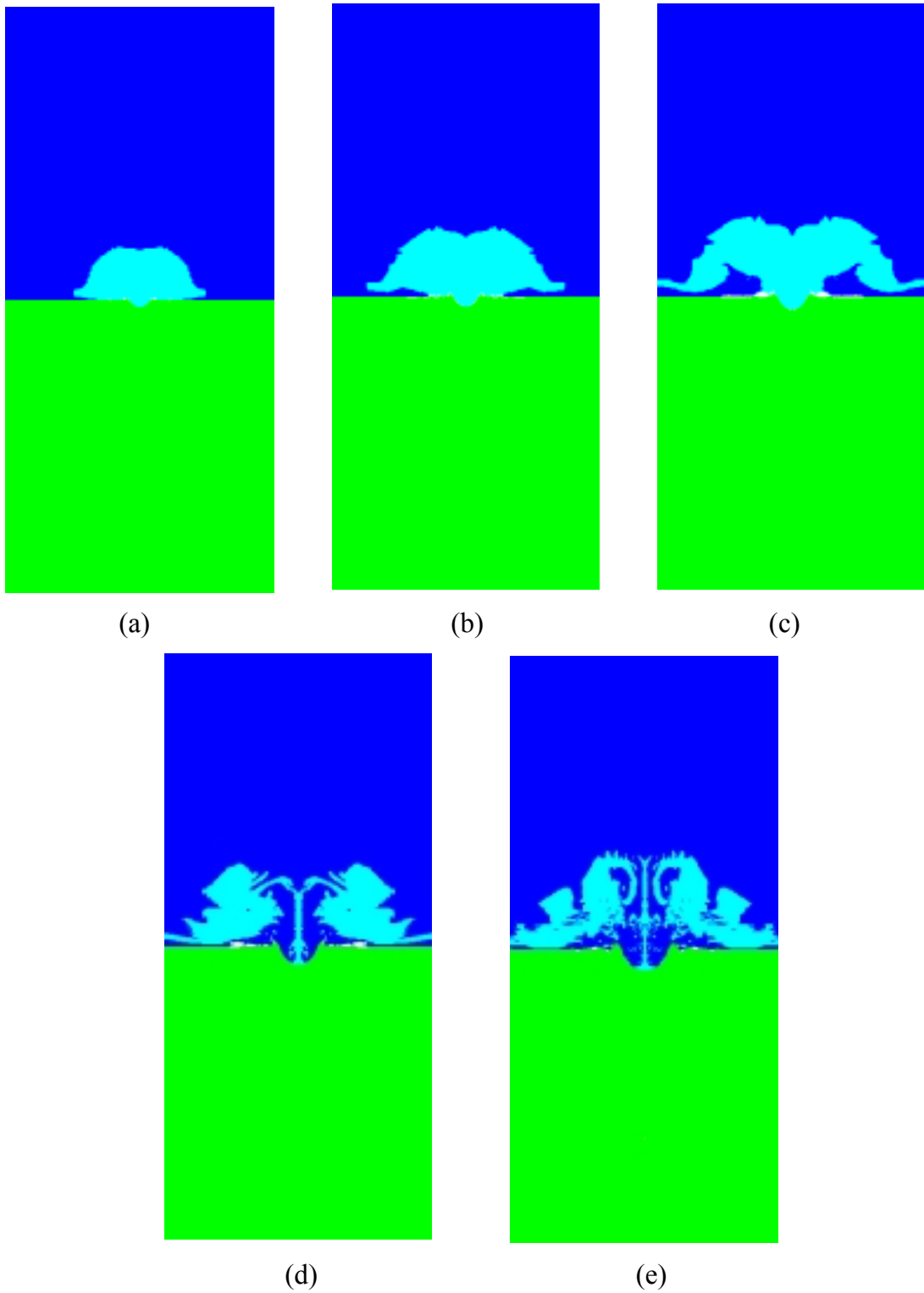


Figure 4: Crater formation. 10 kg TNT on the ground
a) $t=0.5$ ms b) $t=1.1$ ms c) $t=2.0$ ms d) $t=5.2$ ms e) $t=10.0$ ms

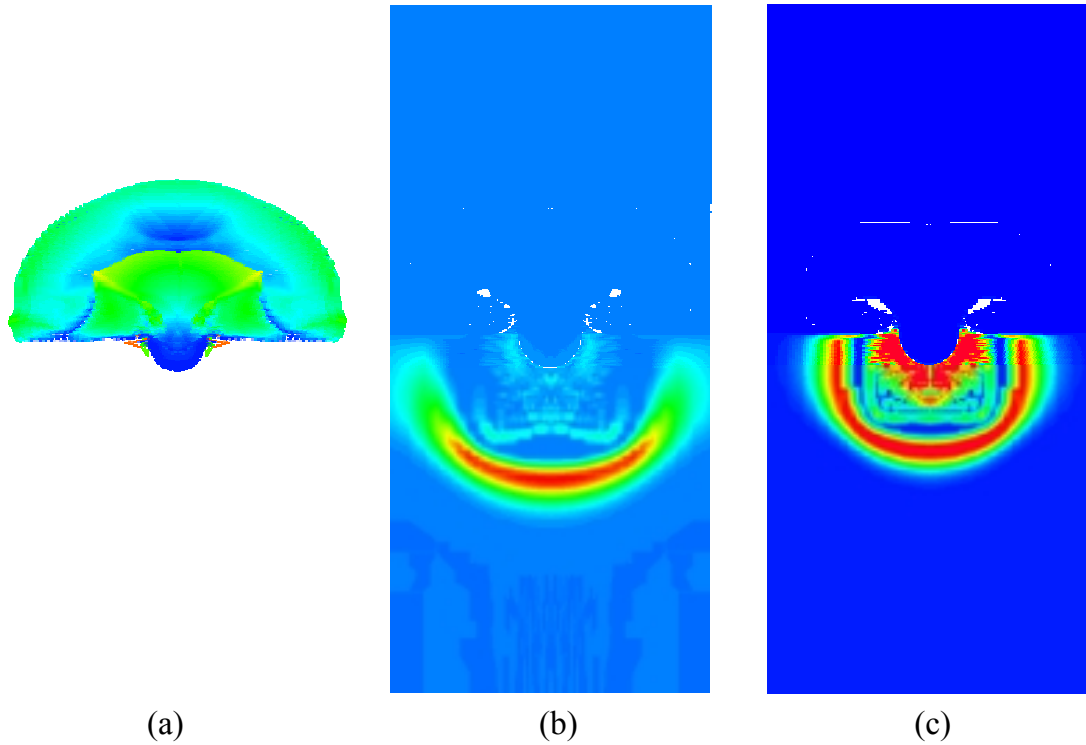
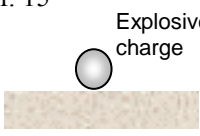
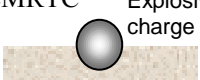


Figure 5: Wave propagation. a) Velocity field in the air b) Pressure contours in the soil c) Von Mises stresses. 50 kg of TNT with the energy release center at the ground level. 1.17 ms

An additional comparison with EMRTC experimental determinations was made. Numerical results and the comparison with experimental ones are presented in Table 2.

Table 2: Apparent crater diameter. Comparison with experimental results


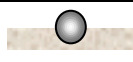
Experimental program	W [kg of TNT]	Exper. results ¹⁵ D[m]	Numer. results D[m]	Numer./Experim.
Ref. 15 	1	0.58	0.60	1.03
	2	0.74	0.72	0.97
	4	0.84	1.03	1.23
	7	1.48	1.12	0.76
	10	1.56	1.54	0.99
EMRTC 	250	3.80	3.94	1.04

It may be observed that a mean difference of about 10% is obtained with respect to experimental results of charges between 1 to 10 kg of TNT and 4% of difference with the experimental result for a greater charge. Obviously, the last value should not be considered in a quantitative form because it is only the comparison of one result, but the qualitative tendency of the numerical model seems to be good both for small and big charges.

4.3 Numerical results

The crater dimensions for explosive charges from 50 to 500 Kg of TNT situated on the ground (case a) and with the energy release center at ground level (case b) are calculated in this section. These charge values were used because they are in the medium range of terrorist attacks to buildings. The range of explosive masses used in terrorist attacks is discussed in some papers (Elliot et al.²⁷, Millington²⁸) and it is strongly dependent on the way the explosive is supposed to have been transported. In order to carry out a comparative analysis, the mass of the explosive is defined by TNT masses. The corresponding masses for other explosives can be obtained through the concept of TNT equivalence (Formby and Wharton²⁹). The results obtained are presented in Table 3.

Table 3: Apparent crater diameter. Numerical results

W [kg of TNT]	a)  D[m]	b)  D[m]	Comparison D _(a) /D _(b)
50	2.10	2.76	0.76
100	2.52	3.06	0.82
150	2.62	3.40	0.77
200	3.06	3.76	0.81
250	3.10	4.14	0.75
300	3.20	4.36	0.73
400	3.40	4.60	0.74
500	4.22	5.30	0.80

It may be observed that the crater is always smaller when the explosive is lying on the ground level than when the energy release center is at ground level. The difference is attributed to the fact that the energy release center is elevated from the ground level in case (a). Nevertheless, the ratio between apparent crater diameters of both cases is almost constant, about 0.77 (coefficient of variation 4.4%), for all the charges studied. The results of this numerical analysis are also plotted in Figure 6 to be compared with experimental ones and empirical equation (2).

In a graphic representing crater diameter as a function of the cubic root of the explosive mass, numerical results are presented in Figure 6 for the cases when the explosive is lying on the ground level (case (a) in Figure 6) and when the energy release center is at the ground level level (case (b) in Figure 6). These results can be approximately represented with two straight lines through the origin. These straight lines are similar to that described in equation (2) that was also included in Figure 6 together with its upper and lower limits. Numerical results (b) for explosions with the energy release center at the ground level and EMRTC experimental result are very close to the lower limit of Equation (2). Another linear approximation must be used for explosives lying on the ground as those simulated in numerical series (a).

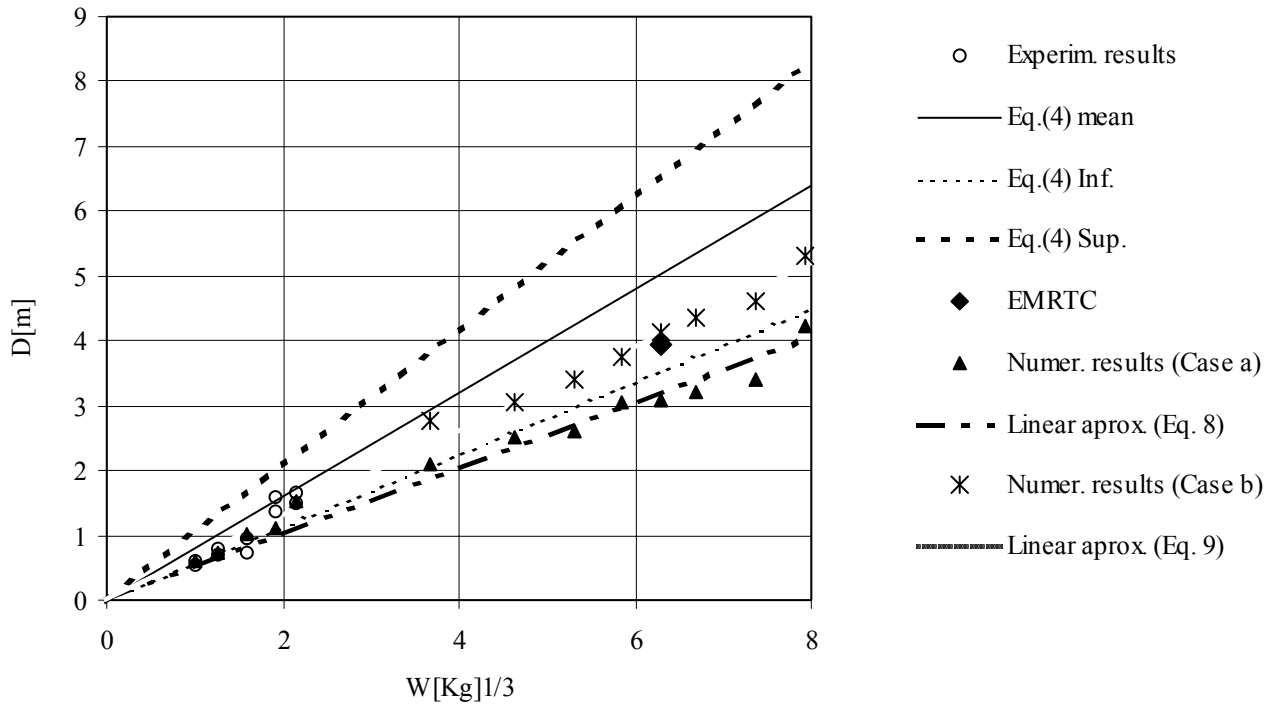


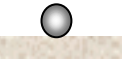
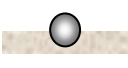
Figure 6: Apparent crater diameter for explosions on and above the ground level

4.4 Variation of soil properties

In order to analyse the influence of soil properties on the size of the craters, additional studies were carried out varying the elastic, failure and yield strength properties.

a) *Shear Modulus*: The value of the shear modulus varied between a wide range: 30 MPa (Soft soil) to 1000 MPa (sound rock). The results are presented in Table 4.

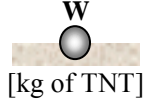
Table 4: Apparent crater diameter. Influence of shear modulus.

W	G	Numer. Results	D_{ref}/D
[kg of TNT]	[MPa]	D[m]	
10 	30	1.564	0.96
	200	1.500	-
	1000	1.388	1.08
250 	30	4.350	0.95
	200	4.140	-
	1000	3.950	1.05

D_{ref} = Diameter corresponding G = 200 MPa

b) *Mass density*: In this case, a wide range was also considered: 1250 kg/m³ to the reference (maximum) density 1950 kg/m³. The results are presented in Table 5.

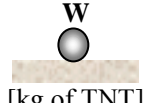
Table 5: Apparent crater diameter. Influence of density.

 W [kg of TNT]	Numerical results		D _(a) /D _(b)
	D[m]		
	a) Mass density 1250 kg/m ³	b) Mass density 1920 kg/m ³	
50	2.76	2.76	1.00
100	3.06	2.92	1.05
150	3.40	3.40	1.00
200	3.76	3.58	1.05
250	4.14	3.78	1.10
300	4.36	3.94	1.11
400	4.60	4.50	1.02
500	5.30	4.60	1.15

It can be seen in Tables 4-5 that the elastic properties of the soil do not affect significantly the diameter of the crater. However, a variation of ± 5% could be obtained in particular cases.

c) *Failure criteria*: The hydro tensile limit varied between -100 to -200 kPa. The results are presented in Table 6.

Table 6: Apparent crater diameter. Influence of Hydro Tensile Limit.

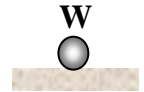
 W [kg of TNT]	Numerical results		D _(a) /D _(b)
	D[m]		
	a) HTL -100 kPa	b) HTL -200 kPa	
50	2.10	2.10	1.00
500	4.22	4.22	1.00

d) *Yield Strength*: Three yield functions were considered and the values are presented in Table 7. The results of the diameter of the crater obtained are shown in Table 8.

Table 7: Yield Functions adopted.

Pressure [kPa]	Yield Stress [kPa]		
	(a)	(b)	(c)
0	6.20 10 ³	1.00 10 ²	2.00 10 ²
3.6 10 ⁴	6.20 10 ³	3.80 10 ²	7.60 10 ²
1.4 10 ⁵	6.20 10 ³	1.14 10 ³	2.28 10 ³
2.7 10 ⁵	6.20 10 ³	1.14 10 ³	2.28 10 ³

Table 8: Apparent crater diameter. Influence of Yield Function.

 W [kg of TNT]	Numerical results. D[m]		
	Yield Function (a)	Yield Function (b)	Yield Function (c)
50	2.10	2.10	2.10
500	4.22	4.22	4.22

It can be seen in Tables 7 and 8 that, when the failure limit and the yield function are changed between reasonable limits, the diameter of the crater remains unchanged.

4.5 Summary of results

From the results obtained, Equations (8) and (9) can be proposed for the prediction of crater dimensions in cases (a) and (b) respectively. These equations represent the linear approximation of numerical result by minimum least-fit squares. The variation of $\pm 5\%$ accounts for the differences between soil properties that could be found in different sites.

Case (a)  $D [m] = 0.51W [Kg]^{1/3} \pm 5\%$ (8)

Case (b)  $D [m] = 0.65W [Kg]^{1/3} \pm 5\%$ (9)

5 CONCLUSIONS

A numerical study of the influence of the soil properties on the size of craters produced by explosive loads was presented in this paper. Materials models and analysis procedures were validated with experimental results. A good agreement was found with existing results for apparent diameters of this type of craters.

The crater diameters for explosive loads from 50 Kg to 500 kg of TNT on the soil surface and with the energy release center at the ground level were obtained. The results obtained confirm that simple empirical linear laws that are proposed in the paper can be used to predict the apparent crater diameter, which is a function of the cubic root of the explosive mass. Moreover, the effect of the elevation of the energy release center when the explosive is on the ground is clearly shown in the numerical results and in the proposed empirical relationship. In order to take into account the particular soil properties of a site, a variation of $\pm 5\%$ in the results should be considered.

Acknowledgements

The financial support of the CONICET (Argentina) and National University of Tucumán is gratefully acknowledged.

6 REFERENCES

- [1]. Baker W.E., Cox P.A., Westine P.S., Kulesz J.J., Strehlow R.A., *Explosion hazards and evaluation*. Elsevier, Amsterdam (1983).
- [2]. Smith PD, Hetherington JG, *Blast and Ballistic Loading of Structures*, Butterworth-Heinemann Ltd, Great Britain. (1994).
- [3]. Ambrosini, RD., Luccioni BM. and Danesi RF. “Craters produced by explosions on the soil surface”, *Mecánica Computacional*, Vol. XXII, pp. 678-692. (2003).
- [4]. Kinney G.F., Graham K.J. *Explosive shocks in air*. 2nd Edition, Springer Verlag, (1985).
- [5]. Persson PA, Holmberg R., Lee J, *Rock blasting and explosives engineering*, CRC Press, USA, (1994).
- [6]. Bull JW, Woodford CH, “Camouflets and their effects on runway supports”, *Computer and Structures*, 69(6), 695-706 (1998).
- [7]. Baker WE, Westine PS, Dodge FT, *Similarity methods in engineering dynamics*. Elsevier, Amsterdam (1991).
- [8]. Melosh HJ, *Impact cratering—A geologic process*. The Clarendon Press, Oxford university press, New York, (1989).
- [9]. Iturrioz I, Riera JD. “Numerical Study of the Effect of Explosives on a Plane Surface”, *XII Congress on Numerical Methods and their Applications*, ENIEF 2001, Arg. 2001.
- [10]. Yang R, Bawden WF, Katsabanis PD. “A New Constitutive Model for Blast Damage”, *Int. J. Rock Mech. Min. Sci. & Geomech. Abstr.*, 33(3), 245-254. (1996).
- [11]. Wu C., Lu Y, Hao H. “Numerical prediction of blast-induced stress wave from large-scale underground explosion”, *International Journal for Numerical and Analytical Methods in Geomechanics*, 28, 93-109. (2004).
- [12]. Wang Z., Lu Y. “Numerical analysis on dynamic deformation mechanism of soils under blast loading”, *Soil Dynamics and Earthquake Engineering*, 23, 705-714. (2003).
- [13]. Zhou XL, Wang JH, Lu JF. “Transient dynamic response of poroelastic medium subjected to impulsive loading”, *Computers and Geotechnics. Technical Note*, 30, 109–120. (2003).
- [14]. Liu L, Katsabanis PD. “Development of a Continuum Damage Model for Blasting Analysis”, *Int. J. Rock Mech. Min. Sci.*, 34(2), 217-231. (1997).
- [15]. Ambrosini, RD., Luccioni BM., Danesi RF., Riera JD. and Rocha MM. “Size of Craters Produced by Explosive Charges on or Above the Ground Surface”, *Shock Waves*, Springer Verlag. 12(1), 69-78, (2002).
- [16]. Baratoux D, Melosh HJ. “The formation of shatter cones by shock wave interference during impacting”. *Earth and Planetary Science Letters*, 216, 43-54. (2003)
- [17]. Nolan MC, Asphaug E, Greenberg R, Melosh HJ. “Impacts on Asteroids: Fragmentation, Regolith Transport, and Disruption.” *Icarus* 153, 1–15, (2001).
- [18]. Pierazzo E, Melosh HJ. “Hydrocode modeling of Chicxulub as an oblique impact event.” *Earth and Planetary Science Letters*, 165, 163-176, (1999).

- [19]. AUTODYN. *Interactive Non-Linear Dynamic Analysis Software*, Version 4.3, User's Manual. Century Dynamics Inc., (2002)
- [20]. Cowler MS, Hancock SL. "Dynamic fluid-structure analysis of shells using the PISCES 2DELK computer code". *5th Int. Conf. on Structural Dynamics in Reactor Technology*, Paper B1/6, (1979).
- [21]. Hancock S. "Finite Difference Equations for PISCES-2DELK", *TCAM-76-2, Physics International*, (1976)
- [22]. Wilkins, ML. "Calculation of Elastic-Plastic Flow", *Methods of Computational Physics*, 3, 211-263 (1964).
- [23]. Youngs, DL. "Time-Dependent Multimaterial Flow with Large Fluid Distortion", *Numerical Methods for Fluid Dynamics*, (1982).
- [24]. Lee, E.L. and Tarver, CM. "Phenomenological Model of Shock Initiation in Heterogeneous Explosives", *Physics of Fluids*, 23(12), 2362-2372 (1980).
- [25]. Ohsaki Y, Iwasaki R. "On dynamic shear moduli and Poisson's ratios of soil deposits." *Soils and Foundations*, 13, 61-73. (1973)
- [26]. Hara A, Ohta T, Niwa M, Tanaka S, Banno T. "Shear modulus and shear strength of cohesive soils". *Soils and Foundations*, 14, 1-12. (1974).
- [27]. Elliot CL., Mays GC. and Smith PD. "The protection of buildings against terrorism and disorder", *Proceedings of Ins. of Civil Engs: Structures & Buildings*, 94, 287-297 (1992).
- [28]. Millington, G. "Discussion of 'The protection of buildings against terrorism and disorder'", *Proc. of Inst. of Civil Engineers: Structures & Buildings*, 104, 343-350 (1994).
- [29]. Formby SA., Wharton RK. "Blast Characteristics and TNT Equivalence Values for Some Commercial Explosives Detonated at Ground Level", *Journal of Hazardous Materials*, 50, 183-198 (1996).